Cost-effective Coherent Systems for Metropolitan Networks

Josep M. Fabrega, Laia Nadal, Michela Svaluto Moreolo
Optical Networks and Systems Department
Centre Tecnològic de Telecomunicacions de Catalunya (CTTC/CERCA)
Castelldefels, Spain
jmfabrega@cttc.es

***Abstract*—Future network services are conceived around the joint use of different heterogeneous resources while combining networking and cloud functions. In order to tackle such a huge challenge, dynamic data plane solutions are needed. In fact, transmission systems need to be agile, programmable, and capable of transmitting large amounts of data dynamically. These transmission systems are expected to be cost/power-effective while covering actual metropolitan networks.**

In this work, we present transmission solutions using coherent detection combined with either direct or external modulation, with special focus on flexible, high capacity and cost-effective systems. The performance of the proposed technologies is evaluated by experiments and careful numerical modeling.

***Index Terms*—Optical networks, fiber optic communications, optical modulation, optical detection**

I. Introduction

Future network services are conceived around the joint use of different heterogeneous resources (including transport, fixed and mobile) in combination with networking and cloud functions. For example, different core functionalities can be hosted in data centers located at different local metro nodes and close to the end users. This entails a huge transformation of the metro/regional network segment [1], [2].

In order to tackle this challenge, dynamic data plane solutions are needed. In fact, transmission systems need to be agile, programmable, and capable of transmitting large amounts of data dynamically, while enabling the suitable allocation and configuration of bandwidth resources accordingly [2].

Among the possible alternatives, the so-called bandwidth/bitrate variable transceivers (BVTs) are the ideal solution, as they can be remotely configured by the control plane for an optimal management of the network resources [3]. In order to reduce the cost as much as possible while being able to keep a high performance in the broad range of connectivity cases, a simple intensity modulation combined with coherent detection has been proposed [4].

In this work, we present intensity modulation transmission using coherent detection combined with either direct or external modulation, with special focus on flexible, high capacity and cost-effectiveness. Precisely, the performance of the proposed transmission scheme is analyzed and evaluated.

work funded in part by the Spanish AURORAS project (RTI2018-099178-B-I00) and the H2020 project PASSION (G.A. 780326).

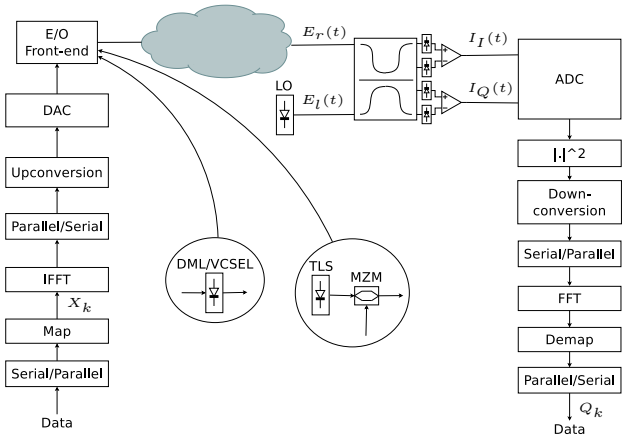

Fig. 1. Generic transceiver scheme.

II. Transceiver Concept

The transceiver is depicted in Fig. 1. At the transmitter, incoming data are parallelized and mapped into the corresponding M-level quadrature amplitude modulation (QAM) constellation. Adaptive bit/power loading can be implemented for either optimizing the performance/capacity of the transceiver [5]. The resulting symbols (X_k) feed an inverse fast Fourier transform (IFFT). Afterwards, the obtained orthogonal frequency-division multiplexing (OFDM) symbols are then serialized and upconverted to an intermediate frequency of half of its bandwidth. The resulting signal is converted to the analog domain by a digital to analog converter (DAC) which drives the transmission optoelectronic (O/E) front-end. Such a front-end can be based either on external modulation, e.g. a Mach-Zehnder modulator (MZM) feeded by a tunable lightwave source (TLS), or a direct modulated laser (DML), e.g. a simple vertical cavity surface emitting laser (VCSEL).

At the receiver, an optoelectronic front-end is proposed, considering a single-polarization scheme based on 90-degree phase diversity. The received signal ($E_r(t)$) is interfered in a 90-degree hybrid by a local laser ($E_l(t)$). At the output of the hybrid, two balanced detection pairs drive a two-channel analog to digital converter (ADC). Next, the square of the modulus of the digital representation of $E_r(t)$ is obtained. The resulting signal is downconverted to baseband, and demodulated following the reversal steps of the OFDM modulation.

978-3-903176-21-8

III. Mathematical model

Let us assume that $E_r(t)$ and $E_l(t)$ can be expressed as

$$E_r(t) = \sqrt{P_r(t)} \exp j(\omega_r t + \phi_r(t)) \quad (1)$$

$$E_l(t) = \sqrt{P_l} \exp j(\omega_l t + \phi_l(t)) \quad (2)$$

being $P_r(t)$ the power of $E_r(t)$, P_l the power of $E_l(t)$, ω_r and ω_l are the central frequencies of $E_r(t)$ and $E_l(t)$, and $\phi_r(t)$ and $\phi_l(t)$ are generic phase shifts of $E_r(t)$ and $E_l(t)$ (e.g. due to phase noise or any other phase distortion).

After balanced detection, we can easily obtain the I and Q components of the mixing between $E_l(t)$ and $E_r(t)$ as

$$I_I(t) = R\sqrt{P_r(t)P_l}\cos\big(\Delta\omega t + \phi_e(t)\big) \quad (3)$$

$$I_Q(t) = R\sqrt{P_r(t)P_l}\sin\big(\Delta\omega t + \phi_e(t)\big) \quad (4)$$

where R is the responsivity of the photodiodes, $\Delta\omega = \omega_r - \omega_l$, and $\phi_e(t) = \phi_r(t) - \phi_l(t)$.

In order to successfully recover $P_r(t)$, we can make

$$I_r(t) = I_I^2(t) + I_Q^2(t) = R^2 P_r(t) P_l \quad (5)$$

So, the detected signal does not depend on the frequency difference nor the relative phase shift between $E_r(t)$ and $E_l(t)$.

In case of having some noise from amplification, the received signal can be rewritten as

$$E_r(t) = E_s(t) + n(t) \quad (6)$$

where $E_s(t)$ is the signal carrying the transmitted data and $n(t)$ is assumed to be a complex Gaussian noise.

At the output of each balanced detector, we will have the beating between noise, useful signal and local laser. Among them the only relevant beating is [6]

$$I_I(t) = R\sqrt{P_s(t)P_l}\cos(\phi) + n_o(t) \quad (7)$$

$$I_Q(t) = R\sqrt{P_s(t)P_l}\sin(\phi) + n_o(t) \quad (8)$$

being $\phi = \Delta\omega t + \phi_e(t)$, and $n_o(t)$ the detected current due to the optical noise. $n_o(t)$ is assumed to be Gaussian noise with 0 mean and power

$$\sigma^2 = \frac{R^2 P_l P_{sa} B_e}{2\mathrm{OSNR} B_o} \quad (9)$$

where P_{sa} is the average received power, B_o is the reference bandwidth for the optical signal to noise ratio (OSNR), e.g. 12.5 GHz, and B_e is the electrical bandwidth of the signal.

So, $I_r(t)$ can be expressed as

$$I_r(t) = I_I^2(t) + I_Q^2(t) = S(t) + N(t) + K(t) \quad (10)$$

where

$$S(t) = R^2 P_s'(t) P_l \quad (11)$$

$$N(t) = R^2 P_{sa} P_l + n_o^2(t) \quad (12)$$

$$K(t) = R\sqrt{P_s'(t)P_l}\big(\cos(\phi) + \sin(\phi)\big) n_o(t) \quad (13)$$

$P_s'(t)$ is an OFDM modulated signal. For simplicity it is assumed to have no DC component, which is taken into account in the noise process $N(t)$. So, we can write

TABLE I
Probability of error for different constellations [8], [9].

Constellation	Probability of error P_e
BPSK	$P_e = \frac{1}{2}\mathrm{erfc}\sqrt{\frac{\mathrm{SNR}}{2}}$
QPSK	$P_e \simeq \frac{1}{2}\mathrm{erfc}\sqrt{\frac{\mathrm{SNR}}{4}}$
MQAM	$P_e = \frac{1}{\log_2 M}\left[1 - \left(1 - \frac{\sqrt{M}-1}{\sqrt{M}}\mathrm{erfc}\sqrt{\frac{3\mathrm{SNR}}{4(M-1)}}\right)^2\right]$

$$P_s'(t) = P_s(t) - P_{sa} = P_{s0}\sum_{k=1}^{N_c}\mathrm{Re}\{X_k \exp(j2\pi f_k t)\} \quad (14)$$

where P_{s0} is the amplitude of the OFDM signal, N_c is the number of subcarriers, $f_k = f_0 + k/T$, f_0 the lowest frequency to be used for OFDM (in our case is set to $f_0 = 0$), $T = N_c/R_s$ the OFDM symbol period, and R_s the symbol rate.

The digital conversion and OFDM processing can be considered as a correlator bank plus sampling. Thus, the demodulated signal can be written as

$$Q_k = \frac{1}{T}\int_0^T I_r(t) T_{k1,2}(t) dt \quad (15)$$

$$= \frac{1}{T}\int_0^T \big[S(t) + N(t) + K(t)\big] T_{k1,2}(t) dt \quad (16)$$

$$= S_k + N_k + K_k \quad (17)$$

with $T_{k1}(t) = \sqrt{\frac{2}{T}}\cos(2\pi f_k t)$, $T_{k2}(t) = -\sqrt{\frac{2}{T}}\sin(2\pi f_k t)$ being the orthogonal functions for generating/detecting the components of each data symbol.

We start with S_k, and find that

$$S_k = \frac{R^2 P_{s0} P_l}{\sqrt{N_c}} X_k \quad (18)$$

whose power can be expressed as $\frac{(R^2 P_{s0} P_l)^2}{N_c}$.

Since $K(t)$ is a cross-product term featuring independent frequency/phase, we assume that it does not match the orthogonality of $T_{k1,2}(t)$ for any k, resulting in $K_k = 0$.

Regarding N_k, note that $N(t)$ follows a non-central Chi-square distribution, since it is a noise process with non-zero mean coming from squaring a Gaussian noise ($n_o(t)$) and adding a certain bias ($R^2 P_{sa} P_l$). This process can be approximated to a Gaussian noise for $R^2 P_{sa} P_l \gg \sigma$ [7]. In that case, the noise power is almost constant in frequency

$$\sigma_N^2 = \frac{2\sigma^4 + 4\sigma^2\big(R^2 P_{sa} P_l\big)^2}{N_c} \quad (19)$$

So, the signal to noise ratio (SNR) can be expressed as

$$\mathrm{SNR} = \frac{(R^2 P_{s0} P_l)^2}{N_c \sigma_N^2} = \frac{(R^2 P_{s0} P_l)^2}{2\sigma^4 + 4\sigma^2\big(R^2 P_{sa} P_l\big)^2} \quad (20)$$

So, we can combine (20) with well-known expressions for obtaining the probability of bit error P_e of different constellations [8], [9], shown in table I.

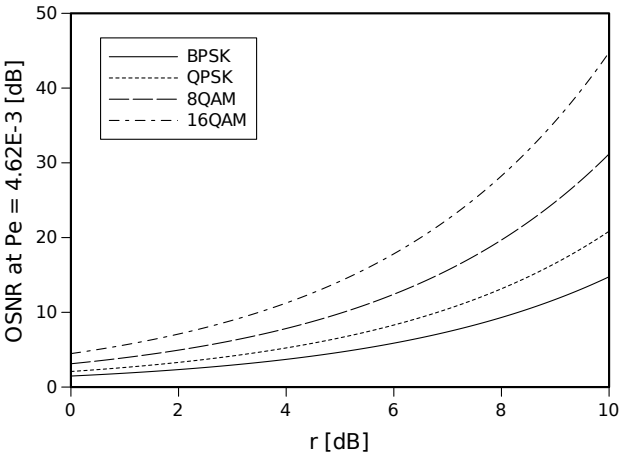

Fig. 2. OSNR at $P_e = 4.62 \cdot 10^{-3}$ as function of $r = P_{sa}/P_{s0}$.

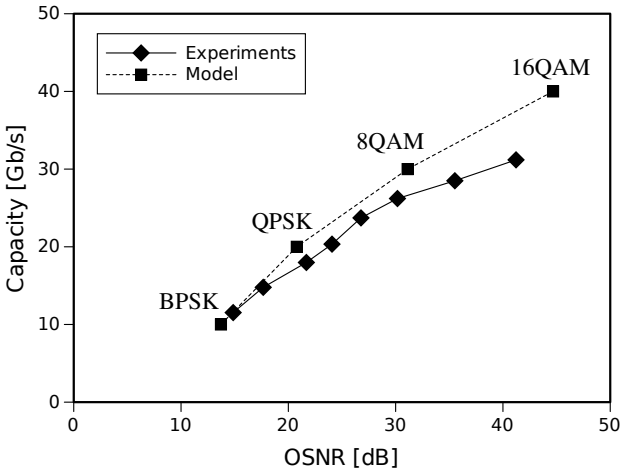

Fig. 3. Capacity as function of OSNR.

TABLE II
VALUES OF THE DIFFERENT PARAMETERS OF THE MODEL.

Parameter	Value	Parameter	Value
P_l	5 dBm	R	0.45 A/W
P_{sa}	5 dBm	B_e	10 GHz
P_{s0}	P_{sa}/r	B_o	12.5 GHz

IV. PERFORMANCE

In order to validate of the model, we use the parameters listed in table II. The objective is to find its agreement with experimental results reported in [4]. There, back-to-back capacity measurements were conducted at the variation of OSNR. In fact, the capacity was optimized using the Levin-Campello algorithm [5] for a bit error ratio (BER) of $4.62 \cdot 10^{-3}$.

First we calculate the OSNR threshold for $P_e = 4.62 \cdot 10^{-3}$ at the variation of $r = P_{sa}/P_{s0}$ for constellations ranging from BPSK up to 16QAM. Results are shown in Fig. 2. As expected, the constellations entailing lower bits per symbol present low OSNR requirement. When the number of constellation points is increased, the OSNR requirement also increases. Also, the required OSNR increases when r increases. In fact, the maximum OSNR needed for $P_e = 4.62 \cdot 10^{-3}$ is 44.67 dB, corresponding to $r = 10$ dB and 16QAM constellation.

We know that capacity of the proposed transmission system is $B_e \cdot \log_2(M)$, being M the number of points of a given constellation. By extracting the suitable OSNR values per constellation from Fig. 2, we can estimate the capacity as function of the OSNR for any given P_e. Please note that the results of such a model constitute an upper theoretical limit to any practical system and have a strong dependence on r. Therefore, characterizing r is crucial for matching the model to any system. For example, in an external modulation like the one depicted in Fig. 1, r can be easily set up with almost no side effects. In case using a DML like a VCSEL, r is set by varying the bias current of the laser. So, optimizing r can also affect other parameters of the transmitter such as the transmission wavelength.

Capacity results are shown in Fig. 3 for $r = 9.5$ dB and $P_e = 4.62 \cdot 10^{-3}$. There we also include the experimental results reported in [4]. Fig. 3 shows that the model matches quite well with the experiments at low capacity, while for a larger capacity there is a difference of ~ 2 Gb/s. In fact, the transmitter employed in [4] was a VCSEL with non-negligible chirp while the model considers ideal intensity modulation.

V. CONCLUSIONS

In this work, we presented intensity modulation transmission solutions using coherent detection combined with either direct or external modulation. A mathematical model for the performance and optimization of the proposed technologies has been proposed and evaluated. Results show good agreement between the model and laboratory experiments.

REFERENCES

[1] Photonics21 Public Private Partnership, "Photonics21 Multiannual Strategic Roadmap 2021-2027," 2019. [Online]. Available: https://www.photonics21.org/download/ppp-services/photonics-downloads/Europes-age-of-light-Photonics-Roadmap-C1.pdf

[2] J. M. Fabrega *et al.*, "Programmable transmission systems using coherent detection enabling multi-Tb/s interfaces for IT-communications convergence in optical networks," in *Metro and Data Center Optical Networks and Short-Reach Links III*, vol. 11308. SPIE, 2020, pp. 65 – 71.

[3] N. Sambo *et al.*, "Next generation sliceable bandwidth variable transponders," *IEEE Communications Magazine*, vol. 53, no. 2, pp. 163–171, Feb. 2015.

[4] M. Svaluto Moreolo *et al.*, "Experimental Assessment of a Programmable VCSEL-based Photonic System Architecture over a Multi-hop Path with 19-Core MCF for Future Agile Tb/s Metro Networks," in *2020 Optical Fiber Communications Conference and Exposition (OFC)*, March 2020, pp. 1–3.

[5] L. Nadal *et al.*, "DMT modulation with adaptive loading for high bit rate transmission over directly detected optical channels," *J. Lightwave Technol.*, vol. 32, no. 21, pp. 3541–3551, Nov 2014.

[6] M. Seimetz, *High-order modulation for optical fiber transmission*, ser. Springer series in optical sciences. Berlin ; New York: Springer, 2009, no. 143, oCLC: ocn297148328.

[7] C. S. Forbes and M. A. Evans, Eds., *Statistical distributions*, 4th ed. Hobokon, NJ: Wiley, 2011, oCLC: 705587087.

[8] J. G. Proakis and M. Salehi, *Digital communications*, 5th ed. Boston, Mass.: McGraw-Hill, 2008, oCLC: 254796470.

[9] A. Goldsmith, *Wireless communications*. Cambridge university press, 2005.